FEBS Letters

FEBS PRESS science publishing by scientists

EDITOR'S CHOICE

ASC-1 transporter-dependent amino acid uptake is required for the efficient thermogenic response of human adipocytes to adrenergic stimulation

Rini Arianti[1,2], Boglárka Ágnes Vinnai[1], Beáta B. Tóth[1], Abhirup Shaw[1,2], Éva Csősz[1], Attila Vámos[1,2], Ferenc Győry[3], Pamela Fischer-Posovszky[4], Martin Wabitsch[4], Endre Kristóf[1] and László Fésüs[1]

1 Department of Biochemistry and Molecular Biology, Faculty of Medicine, University of Debrecen, Hungary
2 Doctoral School of Molecular Cell and Immune Biology, University of Debrecen, Hungary
3 Department of Surgery, Faculty of Medicine, University of Debrecen, Hungary
4 Division of Pediatric Endocrinology and Diabetes, University Medical Center Ulm, Germany

Correspondence
E. Kristóf and L. Fésüs, Department of Biochemistry and Molecular Biology, Faculty of Medicine, University of Debrecen, H-4032 Debrecen, Hungary
Tel: +36 52 416 432
E-mail: kristof.endre@med.unideb.hu (E.K.); fesus@med.unideb.hu (L.F.)

Endre Kristóf and László Fésüs contributed equally to this work.

(Received 20 April 2021, revised 16 June 2021, accepted 28 June 2021, available online 23 July 2021)

doi:10.1002/1873-3468.14155

Edited by Peter Brzezinski

Brown and beige adipocytes dissipate energy by uncoupling protein 1 (UCP1)-dependent and UCP1-independent thermogenesis, which may be utilized to develop treatments against obesity. We have found that mRNA and protein expression of the alanine/serine/cysteine transporter-1 (ASC-1) was induced during adipocyte differentiation of human brown-prone deep neck and beige-competent subcutaneous neck progenitors, and SGBS preadipocytes. cAMP stimulation of differentiated adipocytes led to elevated uptake of serine, cysteine, and glycine, in parallel with increased oxygen consumption, augmented UCP1-dependent proton leak, increased creatine-driven substrate cycle-coupled respiration, and upregulation of thermogenesis marker genes and several respiratory complex subunits; these outcomes were impeded in the presence of the specific ASC-1 inhibitor, BMS-466442. Our data suggest that ASC-1-dependent consumption of serine, cysteine, and glycine is required for efficient thermogenic stimulation of human adipocytes.

Keywords: adipocytes; ASC-1 inhibition; gene expression; obesity; proton leak respiration; thermogenesis; uncoupling protein 1

The activation of nonshivering thermogenesis of brown and beige adipocytes located in either brown or white adipose tissue, respectively, dissipates energy sources to heat. Uncoupling protein 1 (UCP1) plays a major role in their heat generation by creating a proton leak in the inner membrane of mitochondria uncoupling the mitochondrial respiratory chain from ATP synthesis [1]. Both thermogenic adipocytes possess multilocular lipid droplets, high expression of UCP1, and large amounts of mitochondria [2]. Recently, UCP1-independent thermogenesis in beige adipocytes has been described, including a creatine-driven substrate cycle [3,4].

In mice, brown and beige cells have different progenitors and locations exhibiting distinct gene expression and functional signatures [5–8]. It has been

Abbreviations
ASC-1, alanine/serine/cysteine transporter-1; CKB, creatine kinase B; DN, deep neck; ECAR, extracellular acidification rate; FTO, fat mass and obesity-associated; GSH, glutathione; hASCs, human adipose-derived stromal cells; NADPH, nicotinamide adenine dinucleotide phosphate; OCR, oxygen consumption; SC, subcutaneous; SGBS, Simpson-Golabi-Behmel syndrome; TCA, tricarboxylic acid; UCP1, Uncoupling protein 1.

reported that brown adipose tissue adipocytes are derived from myogenic precursors, while beige adipocytes have a common origin with white ones developing from mesenchymal progenitors of white adipose tissue and activated in response to cold and β-adrenergic stimuli, physical exercise, and PPAR-γ stimulation [9,10], which is often referred to as "adipocyte browning." In humans, brown and variably "brownable" adipose tissue depots are interspersed in several anatomical regions, including cervical deep neck (DN), supraclavicular, axillary, paraspinal, and mediastinal depots [11–13]. Unlike in rodents, there is no clear distinction regarding the origin and molecular signature of human brown adipocytes and adipose tissue. Several studies have reported that human brown adipocytes isolated from DN or supraclavicular area resemble murine beige adipocytes [14–17] while others proposed that they closely resemble classic murine brown fat but that some beige adipocytes might also be present in DN [18,19]. Using stromal vascular fractions from brown and white human adipose tissue depots and *ex vivo* brown and white differentiation protocols, adipocyte cultures with high and low proportion of thermogenesis competent cells can be obtained [20–23].

Emerging evidence suggests that beige adipocytes in white adipose tissue persist in a masked form possessing the morphology of white adipocytes [2]. Their activation can quickly occur, usually through adrenergic stimulation, involving inhibition of ongoing mitophagy [23]. Genetic predisposition contributes to the size of the beige cell population; an intronic single nucleotide polymorphism of fat mass and obesity-associated (FTO) gene shifts the balance between white and beige progenitors toward the former [24]. We have recently reported that the FTO status strongly influences the thermogenic potential of neck area adipocytes regardless of type of depot and differentiation protocol [22].

The enhancement of adipocyte thermogenesis can be a promising approach in treating obesity. Therefore, it is important to reveal all molecular elements of thermogenic regulation. Recently, we used high-throughput RNA sequencing technology to analyze global gene expression patterns of *ex vivo* differentiated human DN and subcutaneous (SC) adipocytes that had equal differentiation capacity [22] and found a set of differentially expressed genes when they were compared. One of these genes was *SLC7A10* which showed higher expression in DN-derived adipocytes, particularly when they were differentiated according to a brown protocol. *SLC7A10* encodes the alanine/serine/cysteine transporter-1 (ASC-1) that facilitates the sodium-independent, bidirectional transport of small neutral amino acids, including alanine, serine, cysteine, and glycine. ASC-1 is the main regulator of extracellular D-serine levels in synaptic systems [25]. The ASC-1 transporter was previously listed as a white adipocyte-specific cell surface marker [26]. It has been recently reported that mRNA expression of ASC-1 is high and induced in adipocytes freshly isolated from abdominal subcutaneous and omental white adipose tissue and shows strong inverse correlation with visceral obesity and insulin resistance in humans [27], and it promotes mitochondrial respiration and insulin-stimulated glucose uptake.

Here, we report the induction of ASC-1 during white and brown differentiation of DN and SC-derived neck adipocytes and Simpson-Golabi-Behmel syndrome (SGBS) cells that model beige adipogenic differentiation [28–30]. The presence of a specific ASC-1 inhibitor resulted in decreased serine, cysteine, and glycine consumption during cAMP stimulation of DN-derived white and brown adipocytes with the consequence of decreased UCP1-dependent and UCP1-independent respiration as well as reduced thermogenic gene inductions. cAMP-induced respiratory and gene expression changes could be also reduced by the ASC-1 inhibitor in differentiated adipocytes of SC and SGBS cell origin. The results demonstrate an important role of ASC-1 in regulation of human adipocyte thermogenesis.

Materials and methods

Materials

All chemicals were from Sigma-Aldrich (Munich, Germany) unless stated otherwise.

Ethics statement and obtained tissue samples

Tissue collection was approved by the Medical Research Council of Hungary (20571-2/2017/EKU) followed by the EU Member States' Directive 2004/23/EC on presumed consent practice for tissue collection. All experiments were carried out in accordance with the guidelines of the Helsinki Declaration. Written informed consent was obtained from all participants before the surgical procedure. During thyroid surgeries, a pair of DN and SC adipose tissue samples was obtained to rule out interindividual variations. Patients with known diabetes, malignant tumor, or with abnormal thyroid hormone levels at the time of surgery were excluded. Human adipose-derived stromal cells (hASCs) were isolated from SC and DN fat biopsies as described previously [22,31].

Differentiation and treatment of hASCs and SGBS preadipocytes

White and brown adipocytes were differentiated from stromal vascular fraction of adipose tissue containing hASCs or SGBS preadipocytes according to described protocols [20,21]. Differentiated adipocytes were maintained in DMEM-F12-HAM medium and treated with a single bolus of 500 μM dibutyryl-cAMP (cat#D0627) for 10 h to mimic *in vivo* cold-induced thermogenesis [23]. BMS-466442 (Aobious INC, Gloucester, MA, USA cat#AOB6567) was administered in 100 nM to inhibit ASC-1 transporter activity [32].

Quantification of amino acids and calculation of their uptake by cells

Frozen cell culture supernatants were filtered using 3 kDa filters (Pall Corporation, Port Washington, NY, USA), and then, 10 μL of filtrate was derivatized with AccQ·Tag Ultra Derivatization Kit (Waters, Milford, MA, USA). Chromatographic separation was carried out on H-class UPLC (Waters) using AccQTag Ultra Column (2.1 x 100 mm), AccQTag Eluent A and B, and gradient provided in the AccQTag Ultra Chemistry Kit (Waters). Detection of amino acid derivatives was performed at 260 nm in the PDA detector of the UPLC. Concentration of the amino acids was calculated with the Empower software (Waters) using a 7-point calibration curve.

Flux of amino acids into or from adipocytes was calculated by comparing concentration differences measured at starting and end point of 10 h of dibutyryl-cAMP treatment with or without the presence of ASC-1 inhibitor. The number of cells in wells was calculated using KOVA glasstic slide 10 with grids (Kova International Inc, Garden Grove, CA, USA, cat#K304680) as described (https://www.kovaintl.com/downloads/DI-91064-17).

RNA isolation, RNA-seq analysis, and quantitative real-time PCR (RT-qPCR)

Cells were collected, total RNA was isolated, and RT-qPCR was performed as described previously [28,33]. Gene primers and probes were designed and supplied by Thermo Fisher Scientific (Waltham, MA, USA) as listed in Table S1. Global transcriptome analysis by high-throughput mRNA sequencing was performed on Illumina sequencing platform as detailed in our recent paper [22].

Immunoblotting and densitometry

Immunoblotting and densitometry were carried out as described previously [23]. Antibodies and working dilutions are listed in Table S2.

Oxygen consumption and extracellular acidification rate measurement

Oxygen consumption (OCR) and extracellular acidification rate (ECAR) were measured using an XF96 oximeter (Seahorse Biosciences, North Billerica, MA, USA) as described previously [33]. After recording the baseline OCR, 500 μM dibutyryl-cAMP, 100 nM BMS-466442, or combination of the two compounds was injected to the cells. Then, stimulated OCR was recorded every 30 min. The adipocytes were treated with the creatine analogue 2 mM β-guanidinopropionic acid (β-GPA) which interferes with creatine-driven substrate cycle [3,34]. Proton leak respiration was determined after injecting oligomycin at 2 μM concentration. Cells received a single bolus of antimycin A at 10 μM concentration for baseline correction (measuring nonmitochondrial respiration). The OCR was normalized to protein content.

Statistical analysis

The results are expressed as mean ± SD. Normality of the data was tested by Kolmogorov–Smirnov test. For multiple comparisons of groups, statistical significance was determined by one-way analysis of variance followed by Tukey *post hoc* test. In comparison of two groups, two-tailed paired Student's *t*-test was used. The data were visualized and analyzed by using GraphPad prism 8 (GraphPad Software, San Diego, CA, USA).

Results

Alanine/serine/cysteine transporter-1 is induced in human white and brown adipocytes differentiated from deep neck and subcutaneous progenitors and SGBS cells

In an attempt to extend our knowledge about regulatory mechanism of thermogenesis, we have started to study adipocyte populations differentiated to white and brown cells at the same extent from stromal vascular fraction of paired DN and SC adipose tissue sites of nine donors and compared their global gene expression patterns by global RNA sequencing [22]. We found that according to mRNA expression-based ProFAT and BATLAS scores [35,36], DN-derived brown and even white adipocytes had high browning potential probability compared with SC cells and possessed elevated expression of brown-marker genes (e.g., *UCP1, CKMT1A/B, CPT1A/B, CIDEA, PM20D1, DIO2, LEPR, FABP3*); the expression profile of these genes showed a very similar pattern in the samples according to Pearson's correlation analysis (Fig. S1). Looking for potential thermogenesis

regulators, we found that *UCP1* and the brown-marker genes were clustered with *SLC7A10* which encodes the amino acid transporter ASC-1. *SLC7A10* mRNA was elevated in DN as compared to SC adipocytes with higher levels in brown than in white cells (Fig. 1A). The same expression pattern of *ASC-1* and *UCP1* was observed when we validated the RNA-seq data by RT-qPCR analysis in adipocytes obtained from a separate set of donors (Fig. 1B). We noticed that the expression of *ASC-1* was low in both DN and SC preadipocytes and was induced during the brown and white differentiation process in parallel with various levels of *UCP1* induction. The transporter protein was present in the adipocytes after differentiation and neither the differentiation protocol nor the anatomical origin of the cells resulted in consistently different ASC-1 protein levels (Fig. 1C) while UCP1 levels were higher in DN and brown cells compared with SC and white ones.

We have also investigated the expression of ASC-1 transporter in SGBS cells which can model beige differentiation [28]. It was induced in differentiating SGBS adipocytes (Fig. 1D) and both white and brown cells contained ASC-1 protein with a higher level in the former (Fig. 1E). In accordance with published results, SGBS beige adipocytes, obtained with brown differentiation protocol, showed higher level of *UCP1* mRNA as well as protein expression [28].

Facilitated serine, cysteine, and glycine uptake by adrenergic stimulation of DN adipocytes is decreased in the presence of ASC-1 inhibitor

To learn the functional significance of ASC-1 in adipocytes, we calculated the consumption of alanine, serine, cysteine, and glycine by the differentiated brown and white DN adipocytes after their adrenergic stimulation by the cell-permeable dibutyryl-cAMP for 10 h. We found that serine, cysteine, glycine, and also the ASC-1 substrate threonine were transported at a high basal rate into unstimulated brown and white adipocytes (significantly more serine and cysteine into white than into brown cells), which could be inhibited by the addition of the specific noncompetitive ASC-1 inhibitor, BMS-466442 (Fig. 2), in a nanomolar concentration which was effective in previous cellular experiments [32]. cAMP treatment led to significant facilitation of the uptake of these amino acids, and this was suppressed in the presence of the ASC-1 inhibitor. Interestingly, alanine uptake was low into white adipocytes and brown cells even transported alanine out both in resting and cAMP-stimulated conditions; none of the latter were significantly influenced by the inhibitor treatment. Alanine release may indicate that brown adipocytes degrade amino acids for fueling the tricarboxylic acid (TCA) cycle and convert nitrogen to pyruvate forming alanine as part of a possible glucose/alanine cycle *in vivo* [37]. Since ASC-1 operates preferentially, although not exclusively, in an exchange mode [38], alanine release may allow uptake of more serine, cysteine, and glycine. In this context, we also observed significant release of glutamate which can be transported by ASC-1.

ASC-1 inhibition hinders UCP1-dependent and UCP1-independent oxygen consumption upon cAMP stimulation

Next, we investigated the importance of ASC-1 in thermogenic activation of adipocytes by monitoring oxygen consumption rate and blocking ASC-1 transporter activity by adding the inhibitor, BMS-466442 during short-term adrenergic stimulation. Of note, the inhibitor did not influence mRNA and protein expression of ASC-1 in either the primary or SGBS adipocyte (Fig. S2). As expected, OCR was elevated immediately upon cAMP addition to white and brown DN adipocytes (Fig. 3A) which preserve their thermogenesis potential during differentiation. The respiratory response of the brown adipocytes compared with white ones was higher in accordance with higher expression of *UCP1* and other thermogenesis-related genes [22]. The ASC-1 inhibitor significantly reduced cAMP-stimulated oxygen consumption in both types of adipocytes (Fig. 3A). Basal respiration was not affected by ASC-1 inhibition in spite of the decreased uptake of serine, cysteine, and glycine in resting adipocytes (Fig. 2), showing that the transporter plays a respiration facilitating role during thermogenic activation of adipocytes. To determine the effect of the inhibitor on UCP1-dependent portion of cellular respiration, we injected oligomycin that blocks ATP-synthase activity and makes estimation of UCP1-dependent proton leak possible. This was reduced by the ASC-1 inhibitor in both white and brown cAMP-stimulated DN adipocytes (Fig. 3A) pointing to a significant influence of ASC-1 transported amino acids on mitochondrial proton gradient generation and its uncoupling. Contribution of a UCP1-independent creatine-driven substrate cycle to the stimulated respiration was estimated by applying the creatine analogue, β-GPA, and calculating the consequent reduction in oxygen consumption [3,33]; β-GPA-inhibited portion of respiration was elevated following cAMP treatment, and it could be blunted by the ASC-1 inhibitor in both white and brown DN adipocytes. Non-mitochondrial respiration (Fig. 3A), basal, and cAMP-

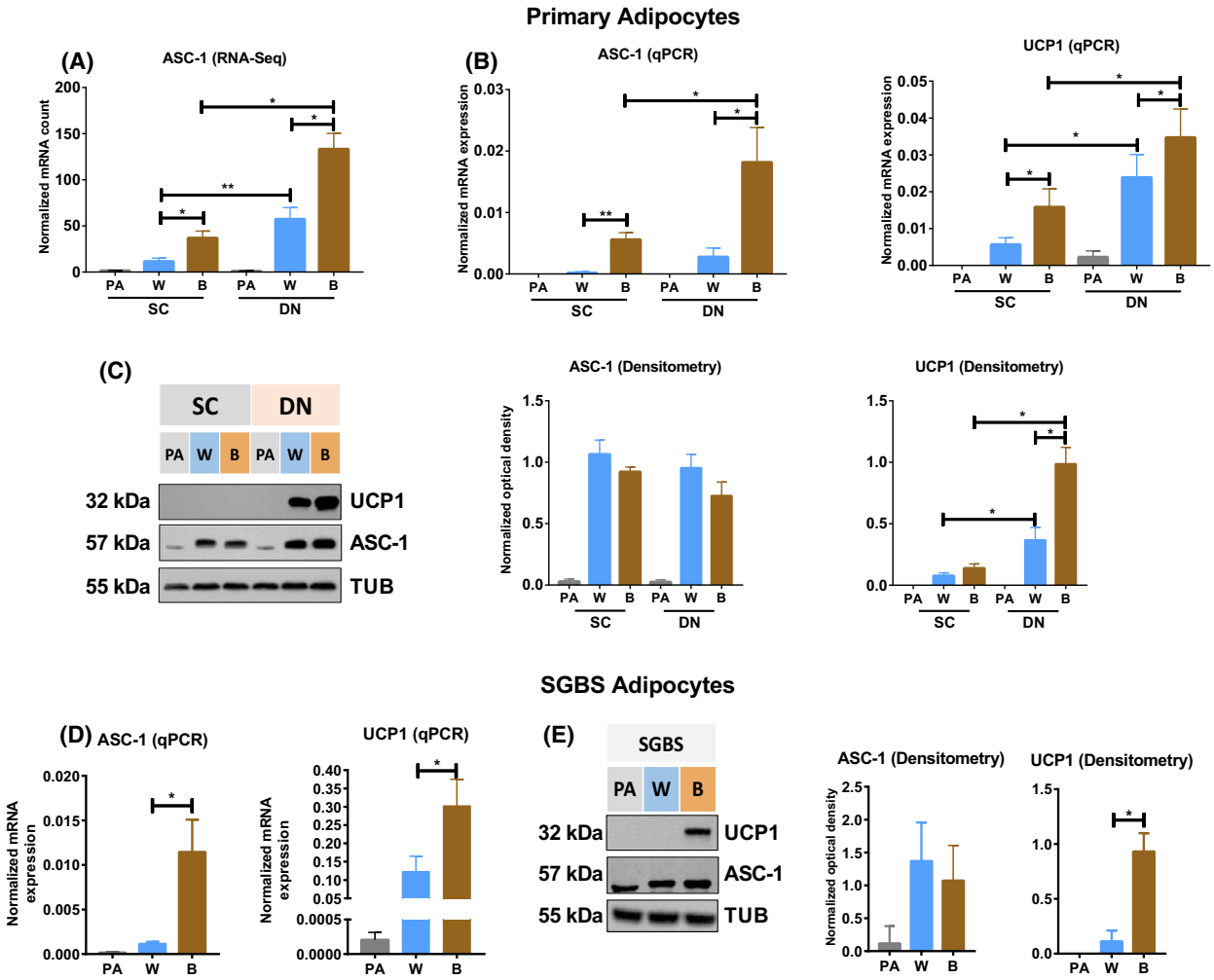

Fig. 1. mRNA and protein expression of alanine/serine/cysteine transporter-1 (ASC-1) in human neck area and Simpson-Golabi-Behmel syndrome (SGBS) adipocytes. (A) ASC-1 mRNA expression determined by RNA-seq. $n = 9$ for all groups. Statistical analysis was performed by one-way ANOVA with the option "each row represents matched, or repeated measures, data." (B) Validation of ASC-1 mRNA expression by RT-qPCR. $n = 6$ for all groups. (C) Detection and quantification of ASC-1 and uncoupling protein 1 (UCP1) by immunoblotting and densitometry. $n = 7$ for all groups. (D) mRNA and (E) protein expression of ASC-1 and UCP1; $n = 5$ for all groups. PA, preadipocytes; W, white; B, brown differentiation. Unless indicated, statistical analysis was performed by paired *t*-test, $^*P < 0.05$, $^{**}P < 0.01$.

stimulated ECAR (Fig. 3B) were not influenced by inhibition of ASC-1.

As we observed UCP1 protein expression in white and brown SC and SGBS adipocytes, we also investigated the respiratory response in these cells. The basal respiration of brown SC and SGBS adipocytes was higher than of white ones (Fig. S3A-B). cAMP increased oxygen consumption in both white and brown SC and SGBS adipocytes. ASC-1 inhibition significantly decreased cAMP-stimulated UCP1-dependent and UCP1-independent (β-GPA-inhibited) oxygen consumption in both white and brown SC and SGBS adipocytes, but did not affect the basal and nonmitochondrial respiration (Fig. S3A-B). The basal and cAMP-stimulated ECARs of SC and SGBS adipocytes were not affected by ASC-1 inhibitor (Fig. S3C). These data suggest that SC neck and SGBS adipocytes also possess thermogenic potential and ASC-1-mediated amino acid transport is needed for its efficient activation.

Inhibition of ASC-1 abrogates the upregulation of thermogenic markers and mitochondrial complexes upon cAMP stimulation

Based on the observed effect of ASC-1 transporter inhibition on cAMP-stimulated respiration of adipocytes,

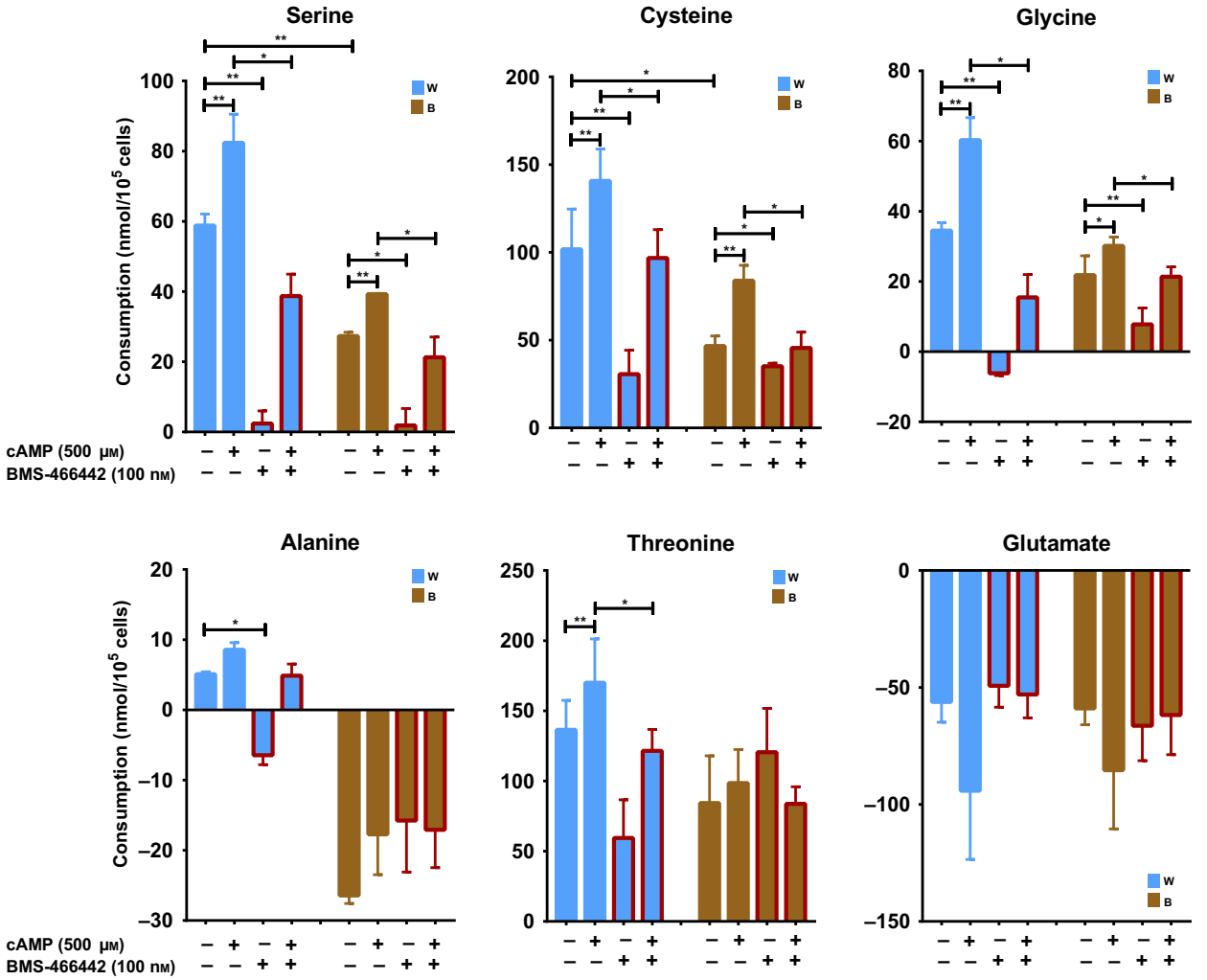

Fig. 2. Effect of 10 h of thermogenic induction and ASC-1 inhibitor (BMS-466442) treatment on serine, cysteine, glycine, alanine, threonine, and glutamate consumption by human deep neck area-derived adipocytes. W, white; B, brown differentiation; $n = 3$ for all groups. Statistical analysis was performed by paired *t*-test, $*P < 0.05$, $**P < 0.01$.

we presumed that induction of thermogenic genes was also affected. DN adipocytes had the tendency to express PGC1α, UCP1, and CKMT2 browning markers at a higher extent than the SC ones (Fig. 4A) as reported previously [22]. As anticipated, cAMP elevated the mRNA and protein expression of these genes in both white and brown SC and DN adipocytes, with some exceptions in white SC cells (Fig. 4B). Inhibition of ASC-1 resulted in reduced cAMP-dependent upregulation of PGC1a, CKMT2, and UCP1 mRNA and protein expression. cAMP could also increase the mRNA and protein expression of the three thermogenic genes in white and brown SGBS adipocytes in most cases and this was also prevented in the presence of the ASC-1 inhibitor (Fig. 4C,D).

We also investigated the effect of ASC-1 inhibitor on other brown/beige adipocyte markers in primary adipocytes. cAMP increased the mRNA expression of *PM20D1* [39], *CKMT1A/B* [3], *ELOVL3* [40], *CITED1* [15], *DIO2* [41], and *TBX1* [16] which was blunted by ASC-1 inhibition (Fig. S4).

In addition to thermogenic markers, we also investigated the effect of ASC-1 transporter inhibitor on protein expression of mitochondrial complex subunits. cAMP treatment elevated the expression of complex I and II subunits in DN (except in some brown cells with already high levels) and partially in SC adipocytes. The elevated levels could be reduced by the addition of the ASC-1 inhibitor (Fig. 5A-C,E). The amount of mitochondrial complex III and V subunits

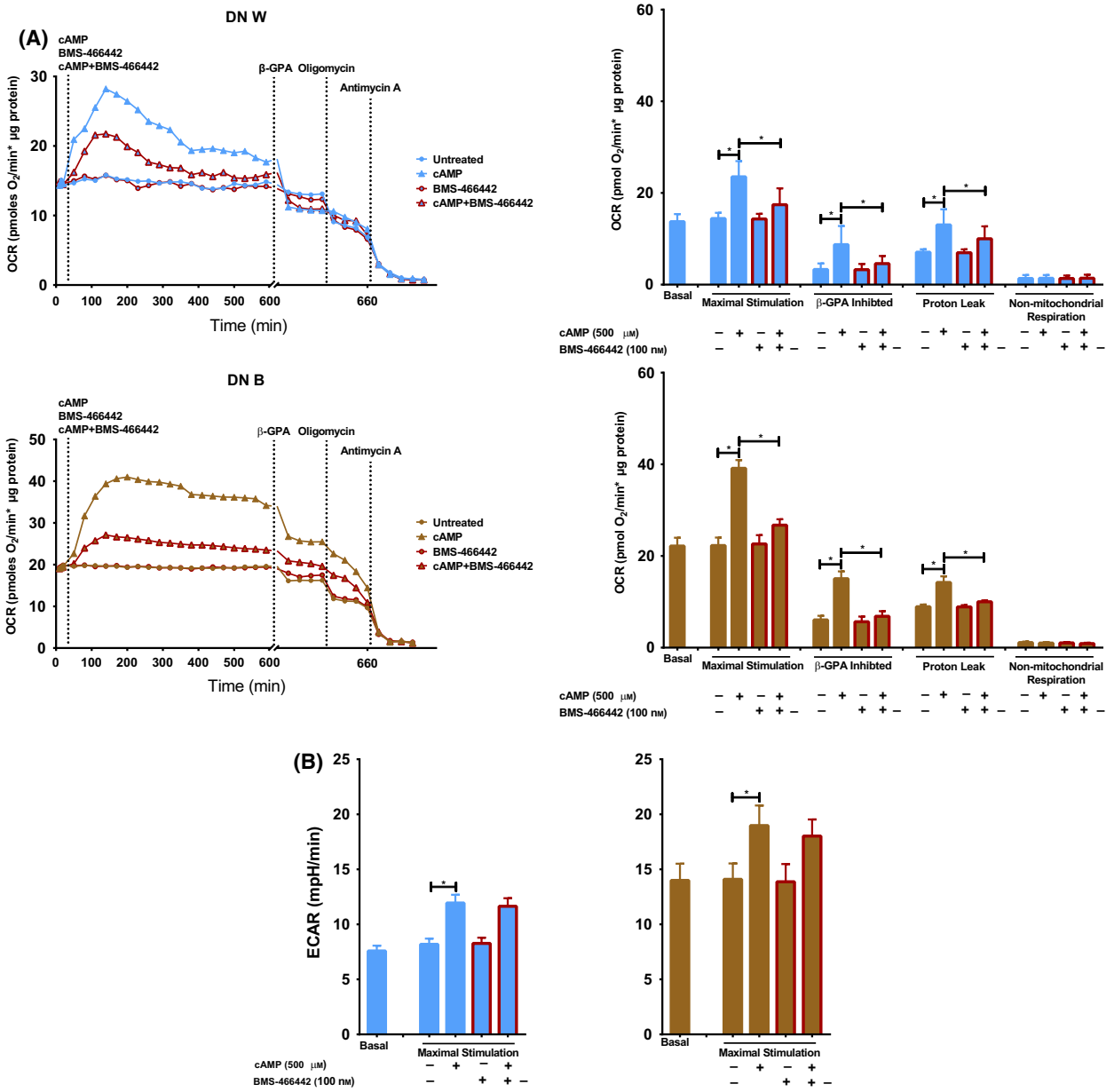

Fig. 3. Effect of ASC-1 inhibitor (BMS-466442) on cAMP-stimulated oxygen consumption rate (OCR) and extracellular acidification rate (ECAR) in human deep neck (DN) white and brown adipocytes. (A) OCR of adipocytes was detected for 10 h following cAMP stimulation without and with ASC-1 inhibition; representative curves of four measurements (left panels). OCR at basal, maximal stimulation, after β-GPA inhibition, oligomycin, and antimycin A addition (right panels) was quantified in adipocytes derived from four independent donors. (B) ECARs of DN white and brown at basal and maximal stimulation; $n = 4$ for all groups. W, white; B, brown differentiation. Statistical analysis was performed by paired *t*-test, $*P < 0.05$, $**P < 0.01$.

was not affected by either cAMP or the inhibitor while complex IV levels in DN cells were decreased by the latter (Fig. 5D,F). cAMP stimulation did not lead to significant increase in mitochondrial complex subunits in either white or brown SGBS adipocyte and ASC-1 inhibition did not have pronounced effects (Fig. S5).

Discussion

SLC transporters act as metabolic gates for the cells and facilitate the transport of important biomolecules such as glucose, amino acids, fatty acids, vitamins, and ions [42]. Thermogenic brown and beige adipocytes utilize glucose and fatty acids in a

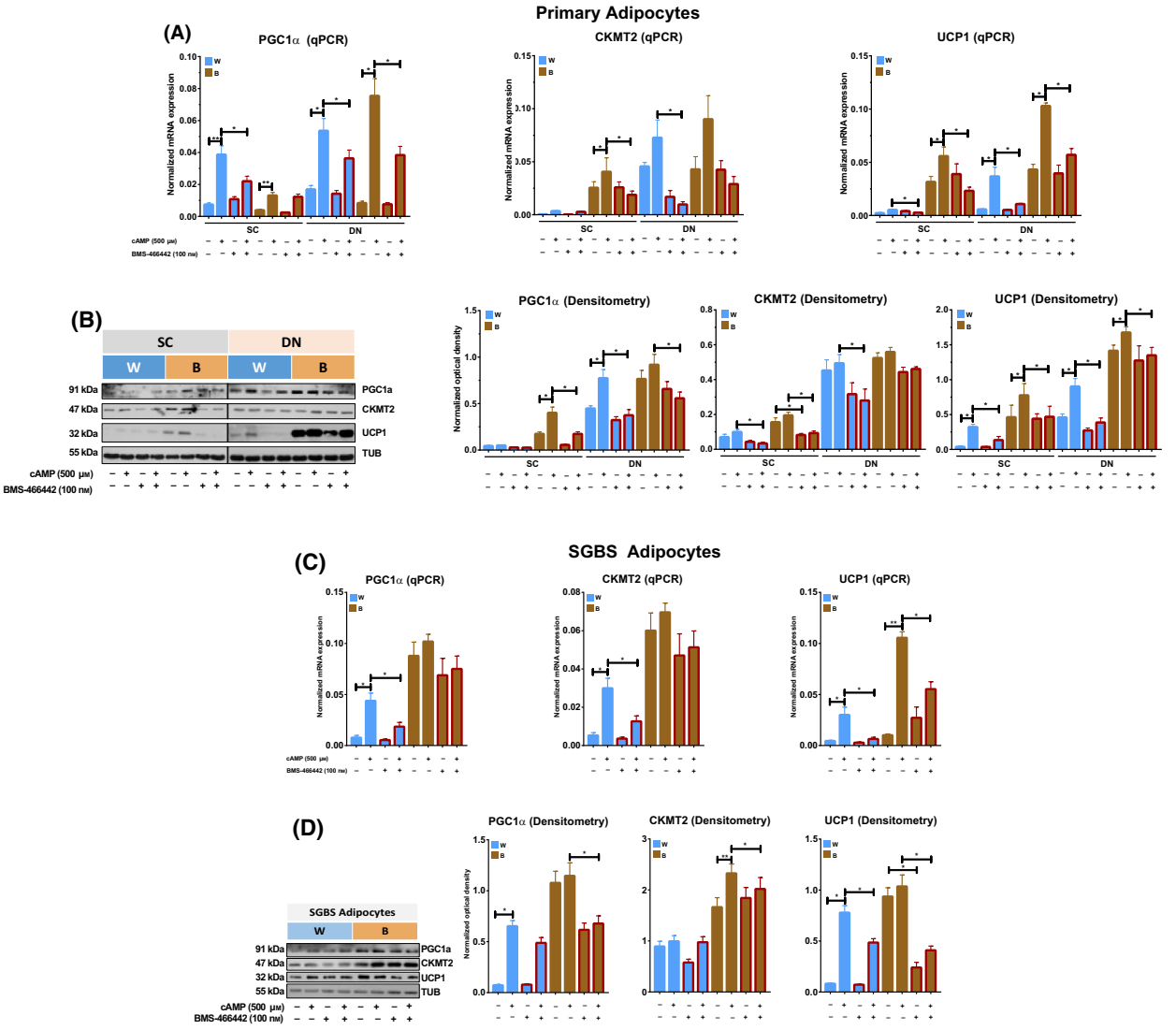

Fig. 4. Effect of ASC-1 inhibitor on the expression of thermogenic marker genes in human primary SC, DN, and SGBS adipocytes. (A-B) mRNA and protein expression of peroxisome proliferator-activated receptor gamma coactivator 1-alpha (PCG1a), creatine kinase, mitochondrial 2 (CKMT2), and uncoupling protein 1 (UCP1) detected by RT-qPCR and immunoblotting in human neck adipocytes. $n = 3$ for all groups. (C–D) mRNA and protein expression of PCG1a, CKMT2, and UCP1 detected by RT-qPCR and immunoblotting in SGBS adipocytes. $n = 3$ for all groups. W, white; B, brown differentiation. Statistical analysis was performed by paired *t*-test, $*P < 0.05$, $**P < 0.01$.

significant proportion as fuels to generate heat and SLC transporters mediate their uptake *via* the glucose transporter-4, encoded by *SLC2A4*, and the fatty acid transporter-1, encoded by *SLC27A1* [43,44]. Brown adipose tissue can actively oxidize branched-chain amino acids during cold-induced thermogenesis [45]; however, the role of amino acid influx in the metabolism and regulation of thermogenic adipocytes has not been fully investigated so far. The data presented here have revealed the importance of the alanine, serine, cysteine, glycine transporter ASC-1 (encoded by *SLC7A10*), induced during adipocyte differentiation, in stimulated thermogenesis of human adipocytes. Inhibition of ASC-1 during cAMP treatment prevented efficient response of highly thermogenic DN-derived brown and white adipocytes (with a mixed population of brown and beige cells) as well as lower thermogenesis competent adipocyte populations of subcutaneous origin which contain beige cells.

ASC-1 mRNA was induced and expressed at a greater extent in DN and SC brown adipocytes as

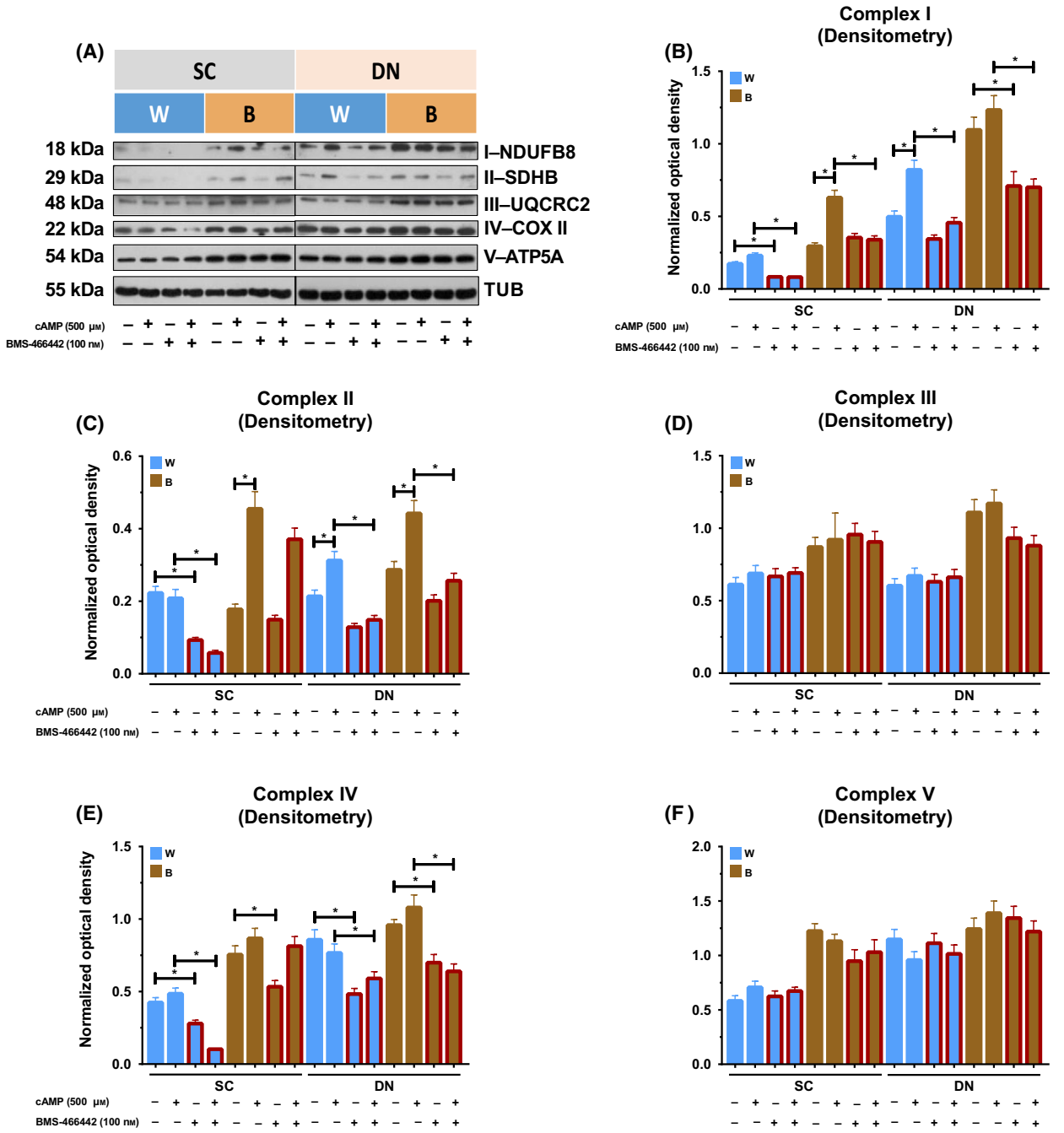

Fig. 5. Effect of ASC-1 inhibitor on the protein expression of mitochondrial complex subunits in primary SC and DN adipocytes. (A) Expression of mitochondrial complex subunits detected by immunoblotting. (B-F) Quantification of complex I-V immunoblotting by densitometry; $n = 3$. W, white; B, brown differentiation. Statistical analysis was performed by paired *t*-test, $*P < 0.05$

compared to white ones, similarly to UCP1 (Fig. 1A, B). At the protein level, ASC-1 expression was either not different or moderately higher in white as compared to brown adipocytes of DN and SC origin (Fig. 1C). ASC-1 was described earlier as a cell surface marker of white adipocytes in humans and mice [26,46]. In mice, its presence in a subpopulation of subcutaneous preadipocytes of adolescent adipose tissue and in differentiating preadipocyte cell lines could even inhibit beige differentiation [47]. In a human study, slightly more ASC-1 mRNA was detected in SC white tissue samples obtained by needle biopsies from

the neck than in DN brown samples [36] and this was reflected in the ASC-1 protein levels we found in SC and DN tissue lysates (Fig. S6). On the other hand, ASC-1 mRNA was expressed at the same level in white and brown adipocytes differentiated from human SC- and DN-derived immortalized preadipocyte clones [26]. Regarding our observations, SC, DN, and SGBS brown differentiated adipocytes had higher ASC-1 mRNA and either the same or moderately less ASC-1 protein levels compared to white ones and the presence of ASC-1 did not suppress thermogenic activity. Sufficient transporter capacity was available in both adipocyte types for cAMP-stimulated increase in serine, cysteine, and glycine influx during elevated UCP1-dependent OCR (Figs 2 and 3).

The extra need of adipocytes for serine, cysteine, and glycine became apparent when we monitored their cAMP-stimulated OCR in the presence of the selective ASC-1 inhibitor, BMS-455442. While the basal OCR was not affected by the inhibitor, it strongly reduced maximal OCR elicited by cAMP in all adipocyte types studied. We found that proton leak respiration, which reflects the abundance and activity of UCP1 in brown or masked beige adipocytes, and activation of the creatine-driven substrate cycle were mainly responsible for the observed OCR burst upon cAMP stimulation of adipocytes. Both were inhibited in the presence of the compound BMS-455442, clearly demonstrating that ASC-1-mediated amino acid uptake is required for the thermogenic response of adipocytes (Figs 3A and S3A,B). Although we have originally assumed that cAMP stimulates serine, cysteine, and glycine uptake through ASC-1, the amino acid consumption data suggest that cAMP activates other transporters for these amino acids. However, ASC-1-mediated basic transport has a critical role in the respiration and gene induction response to thermogenic stimulation since the presence of the ASC-1 inhibitor led to suppression of both.

Serine is an important metabolic source to generate one-carbon units in mammalian cells [48] *via* its breakdown by serine hydroxymethyltransferases. The metabolism of one-carbon units has a functional interaction with the mitochondrial oxidative phosphorylation (OXPHOS) system that is crucial for ATP and heat generation in mammalian cells [49]. We found that mitochondrial OXPHOS system was affected by the inhibition of ASC-1 activity as cAMP-induced elevation of mitochondrial complex I and II subunit protein expression was blunted by the ASC-1 inhibitor (Fig. 5). One-carbon units are also required for the transsulfuration pathway during glutathione (GSH) synthesis as a response to oxidative stress [50]. Serine treatment in mice diminishes oxidative stress by enhancing GSH synthesis and lowers the production of hepatic reactive oxygen species [51]. Serine can also be a main source of nicotinamide adenine dinucleotide phosphate (NADPH) which is required for the reduction of oxidized GSH [52,53].

Short-term adrenergic stimulation of differentiated DN adipocytes leads to the upregulation of thermogenic genes, such as *UCP1* and *PGC1α*. This response was also reduced by ASC-1 inhibitor in both white and brown human SC, DN, and SGBS adipocytes (Fig. 4). Furthermore, we found that the cAMP-stimulated mRNA expression of additional browning genes, such as *ELOVL3*, *DIO2*, and *CITED1*, was also attenuated by the ASC-1 inhibitor. *ELOVL3* is more expressed in brown adipose tissue upon cold exposure [54] and defects in this gene lead to the decreased level of long-chain fatty acids which activate UCP1. DIO2 is highly expressed in brown adipocytes, and its depletion leads to the downregulation of lipolysis and adaptive thermogenesis [55]. CITED1, a beige-selective transcription factor, is highly expressed in human browning cells [15].

Several studies have reported UCP1-independent thermogenesis in browning cells utilizing a creatine futile cycle [3], calcium cycling [4], and uncoupling by N-acyl amino acids [38]. The inhibition of ASC-1 reduced the UCP1-independent thermogenesis mediated by the creatine-driven substrate cycle (Figs 3A and S4A,B). In addition, cAMP-induced upregulation of CKMT2 and CKMT1a/b was also reduced by the ASC-1 inhibitor. CKMT1a/b and CKMT2, the mitochondrial creatine kinases, phosphorylate creatine generating phosphocreatine [3] to which creatine kinase B (CKB) can also contribute [56]. Three types of amino acids methionine, glycine, and arginine are required for creatine synthesis [57]. The interruption of glycine influx by ASC-1 inhibitor may prevent increased creatine synthesis. In addition, ASC-1 inhibition also reduced cAMP-stimulated mRNA expression of *PM20D1* in the adipocytes; PM20D1 regulates the synthesis of the endogenous uncoupler N-lipidated/N-fatty-acyl amino acids, and it was found enriched in brown adipose tissue where it contributes to energy expenditure [38].

ASC-1 has been recently identified as a novel regulator of energy metabolism in white adipocytes enhancing their mitochondrial respiration and preventing development of adipocyte hypertrophy and insulin resistance [27]; a major part of supporting evidence was obtained by applying the same ASC-1 inhibitor, BMS-466442, that we have used in the work presented here. The significant role of ASC-1 in controlling

obesity has been also underlined by the observation in multiple cohorts that its adipose tissue expression is inversely correlated with visceral adiposity and insulin resistance [27]. The capacity to waste energy through thermogenesis by brown and beige adipocytes is low in obese individuals [58,59], particularly in those who carry the FTO rs1421085 obesity-risk allele [24]. Based on our presented data, it can be assumed that the decreased expression of ASC-1 in hypertrophic white adipose tissue of obese individuals may also result in a reduced thermogenesis response of masked beige cells which contribute to excess energy storage, lipid accumulation, and obesity. This might, at least partially, explain the fact that obese individuals possess high amounts of brownable but thermogenically not active fat [13]. Consequently, stimulation of ASC-1 expression in adipose tissue of obese patients and, thereby, facilitation of its beneficial effect on overall energy balance [27] and thermogenic responsiveness may have therapeutic value.

Acknowledgements

We thank Jennifer Nagy for technical assistance and Dr. Károly Jambrovics for help in cell analysis. This research was funded by the European Union and the European Regional Development Fund (GINOP-2.3.2-15-2016-00006), the European Union and the European Social Fund (EFOP-3.6.3-VEKOP-16-2017-00009), and the National Research, Development and Innovation Office (NKFIH-FK131424 and K129139) of Hungary. EK was supported by the János Bolyai Fellowship of the Hungarian Academy of Sciences and the ÚNKP-20-5 New National Excellence Program of the Ministry for Innovation and Technology from the source of the National Research, Development and Innovation Fund. BÁV was supported by the ÚNKP-20-2-I New National Excellence Program of the Ministry for Innovation and Technology from the source of the National Research, Development and Innovation Fund. PF-P was funded by the German Research Association (Fi1700/7-1).

Author contributions

LF and RA conceived and designed the experiments with contributions from EK. RA, BÁV, and EK performed the experiments. BBT analyzed the RNA-seq data. FGy provided tissue samples, PF-P and MW provided SGBS cells. ECs carried out measurement of amino acid concentrations. AS and AV generated primary cell cultures for the experiments. RA and LF wrote the manuscript with inputs from EK and BBT.

Data accessibility

RNA-seq data were deposited in the Sequence Read Archive (SRA) database [https://www.ncbi.nlm.nih.gov/sra] under accession number PRJNA607438. Other data that support the findings of this study are available from the corresponding authors [fesus@med.unideb.hu, kristof.endre@med.unideb.hu] upon reasonable request.

References

1 Chouchani ET, Kazak L and Spiegelman BM (2019) New advances in adaptive thermogenesis: UCP1 and beyond. *Cell Metab* **29**, 27–37.
2 Kajimura S, Spiegelman BM and Seale P (2015) Brown and beige fat: physiological roles beyond heat generation. *Cell Metab* **22**, 546–559.
3 Kazak L, Chouchani ET, Jedrychowski MP, Erickson BK, Shinoda K, Cohen P, Vetrivelan R, Lu GZ, Laznik-Bogoslavski D, Hasenfuss SC *et al.* (2015) A creatine-driven substrate cycle enhances energy expenditure and thermogenesis in beige fat. *Cell* **163**, 643–655.
4 Ikeda K, Kang Q, Yoneshiro T, Camporez JP, Maki H, Homma M, Shinoda K, Chen Y, Lu X, Maretich P *et al.* (2017) UCP1-independent signaling involving SERCA2b-mediated calcium cycling regulates beige fat thermogenesis and systemic glucose homeostasis. *Nat Med* **23**, 1454–1465.
5 Gesta S, Tseng YH and Kahn CR (2007) Developmental origin of fat: tracking obesity to its source. *Cell* **131**, 242–256.
6 Berry DC, Stenesen D, Zeve D and Graff JM (2013) The developmental origins of adipose tissue. *Development* **140**, 3939–3949.
7 Sanchez-Gurmaches J and Guertin DA (2014) Adipocytes arise from multiple lineages that are heterogeneously and dynamically distributed. *Nat Commun* **5**, 4099.
8 Ikeda K, Maretich P and Kajimura S (2018) The Common and Distinct Features of Brown and Beige Adipocytes. *Trends Endocrinol Metab* **29**, 191–200.
9 Lee YH, Petkova AP, Mottillo EP and Granneman JG (2012) In vivo identification of bipotential adipocyte progenitors recruited by β3-adrenoceptor activation and high-fat feeding. *Cell Metab* **15**, 480–491.
10 Wang QA, Tao C, Gupta RK and Scherer PE (2013) Tracking adipogenesis during white adipose tissue development, expansion and regeneration. *Nat Med* **19**, 1338–1344.
11 Cypess AM, Lehman S, Williams G, Tal I, Rodman D, Goldfine AB, Kuo FC, Palmer EL, Tseng YH, Doria A *et al.* (2009) Identification and importance of brown adipose tissue in adult humans. *N Engl J Med* **360**, 1509–1517.

12 Virtanen KA, Lidell ME, Orava J, Heglind M, Westergren R, Niemi T, Taittonen M, Laine J, Savisto NJ, Enerbäck S *et al.* (2009) Functional brown adipose tissue in healthy adults. *N Engl J Med* **360**, 1518–1525.
13 Leitner BP, Huang S, Brychta RJ, Duckworth CJ, Baskin AS, McGehee S, Tal I, Dieckmann W, Gupta G, Kolodny GM *et al.* (2017) Mapping of human brown adipose tissue in lean and obese young men. *Proc Natl Acad Sci USA* **114**, 8649–8654.
14 Lee P, Werner CD, Kebebew E and Celi FS. (2014). Functional thermogenic beige adipogenesis is inducible in human neck fat. *Int J Obes* **38**, 170–176.
15 Sharp LZ, Shinoda K, Ohno H, Scheel DW, Tomoda E, Ruiz L, Hu H, Wang L, Pavlova Z, Gilsanz V *et al.* (2012) Human BAT possesses molecular signatures that resemble beige/brite cells. *PLoS ONE* **7**, e49452.
16 Wu J, Boström P, Sparks LM, Ye L, Choi JH, Giang AH, Khandekar M, Virtanen KA, Nuutila P, Schaart G *et al.* (2012) Beige adipocytes are a distinct type of thermogenic fat cell in mouse and human. *Cell* **150**, 366–376.
17 Shinoda K, Luijten IH, Hasegawa Y, Hong H, Sonne SB, Kim M, Xue R, Chondronikola M, Cypess AM, Tseng YH *et al.* (2015) Genetic and functional characterization of clonally derived adult human brown adipocytes. *Nat Med* **21**, 389–394.
18 Jespersen NZ, Larsen TJ, Peijs L, Daugaard S, Homøe P, Loft A, de Jong J, Mathur N, Cannon B, Nedergaard J *et al.* (2013) A classical brown adipose tissue mRNA signature partly overlaps with brite in the supraclavicular region of adult humans. *Cell Metab* **17**, 798–805.
19 Sanchez-Gurmaches J, Hung CM and Guertin DA (2016) Emerging complexities in adipocyte origins and identity. *Trends Cell Biol* **26**, 313–326.
20 Elabd C, Chiellini C, Carmona M, Galitzky J, Cochet O, Petersen R, Pénicaud L, Kristiansen K, Bouloumié A, Casteilla L *et al.* (2009) Human multipotent adipose-derived stem cells differentiate into functional brown adipocytes. *Stem cells* **27**, 2753–2760.
21 Kristóf E, Doan-Xuan QM, Bai P, Bacso Z and Fésüs L (2015) Laser-scanning cytometry can quantify human adipocyte browning and proves effectiveness of irisin. *Sci Rep* **5**, 12540.
22 Tóth BB, Arianti R, Shaw A, Vámos A, Veréb Z, Póliska S, Győry F, Bacso Z, Fésüs L and Kristóf E (2020) FTO intronic SNP strongly influences human neck adipocyte browning determined by tissue and PPARγ specific regulation: a transcriptome analysis. *Cells* **9**, 987.
23 Szatmári-Tóth M, Shaw A, Csomós I, Mocsár G, Fischer-Posovszky P, Wabitsch M, Balajthy Z, Lányi C, Győry F, Kristóf E *et al.* (2020) Thermogenic activation downregulates high mitophagy rate in human masked and mature beige adipocytes. *Int J Mol Sci* **21**, 6640.
24 Claussnitzer M, Dankel SN, Kim KH, Quon G, Meuleman W, Haugen C, Glunk V, Sousa IS, Beaudry JL, Puviindran V *et al.* (2015) FTO Obesity variant circuitry and adipocyte browning in humans. *N Engl J Med* **373**, 895–907.
25 Rutter AR, Fradley RL, Garrett EM, Chapman KL, Lawrence JM, Rosahl TW and Patel S (2007) Evidence from gene knockout studies implicates Asc-1 as the primary transporter mediating d-serine reuptake in the mouse CNS. *Eur J Neuorsci* **25**, 1757–1766.
26 Ussar S, Lee KY, Dankel SN, Boucher J, Haering MF, Kleinridders A, Thomou T, Xue R, Macotela Y, Cypess AM *et a*l. (2014) ASC-1, PAT2, and P2RX5 are cell surface markers for white, beige, and brown adipocytes. *Sci Transl Med* **6**, 247ra103.
27 Jersin RÅ, Tallapragada D, Madsen A, Skartveit L, Fjære E, McCann A, Dyer L, Willems A, Bjune JI, Bjune MS *et al.* (2021) Role of the neutral amino acid transporter SLC7A10 in Adipocyte lipid storage, obesity, and insulin resistance. *Diabetes* **70**, 680–695.
28 Klusóczki Á, Veréb Z, Vámos A, Fischer-Posovszky P, Wabitsch M, Bacso Z, Fésüs L and Kristóf E (2019) Differentiating SGBS adipocytes respond to PPARγ stimulation, irisin and BMP7 by functional browning and beige characteristics. *Sci Rep* **9**, 5823.
29 Wabitsch M, Brenner RE, Melzner I, Braun M, Möller P, Heinze E, Debatin KM and Hauner H (2001) Characterization of a human preadipocyte cell strain with high capacity for adipose differentiation. *Int J Obes Relat Metab Disord* **25**, 8–15.
30 Fischer-Posovszky P, Newell FS, Wabitsch M and Tornqvist HE (2008) Human SGBS cells - a unique tool for studies of human fat cell biology. *Obesity facts* **1**, 184–189.
31 Kristóf E, Klusóczki Á, Veress R, Shaw A, Combi ZS, Varga K, Győry F, Balajthy Z, Bai P, Bacso Z *et al.* (2019) Interleukin-6 released from differentiating human beige adipocytes improves browning. *Exp Cell Res* **377**, 47–55.
32 Brown JM, Hunihan L, Prack MM, Harden DG, Bronson J, Dzierba CD, Gentles RG, Hendricson A, Krause R, Macor JE *et al.* (2014) In vitro Characterization of a small molecule inhibitor of the alanine serine cysteine transporter -1 (SLC7A10). *J Neurochem* **129**, 275–283.
33 Kristóf E, Doan-Xuan QM, Sárvári AK, Klusóczki Á, Fischer-Posovszky P, Wabitsch M, Bacso Z, Bai P, Balajthy Z and Fésüs L (2016) Clozapine modifies the differentiation program of human adipocytes inducing browning. *Transl Psychiat* **6**, e963.
34 Fitch CD and Chevli R (1980) Inhibition of creatine and phosphocreatine accumulation in skeletal muscle and heart. *Metab Clin Exp* **29**, 686–690.
35 Cheng Y, Jiang L, Keipert S, Zhang S, Hauser A, Graf E, Strom T, Tschöp M, Jastroch M and Perocchi F

(2018) Prediction of adipose browning capacity by systematic integration of transcriptional profiles. *Cell Rep* **23**, 3112–3125.
36 Perdikari A, Leparc GG, Balaz M, Pires ND, Lidell ME, Sun W, Fernandez-Albert F, Müller S, Akchiche N, Dong H *et al.* (2018) BATLAS: deconvoluting brown adipose tissue. *Cell Rep* **25**, 784–797.
37 Felig P (1973) The glucose-alanine cycle. *Metab Clin Exp* **22**, 179–207.
38 Fukasawa Y, Segawa H, Kim JY, Chairoungdua A, Kim DK, Matsuo H, Cha SH, Endou H and Kanai Y (2000) Identification and characterization of a Na (+)-independent neutral amino acid transporter that associates with the 4F2 heavy chain and exhibits substrate selectivity for small neutral D- and L-amino acids. *J Biol Chem* **275**, 9690–9698.
39 Long JZ, Svensson KJ, Bateman LA, Lin H, Kamenecka T, Lokurkar IA, Lou J, Rao RR, Chang MR, Jedrychowski MP *et al.* (2016) The secreted enzyme PM20D1 Regulates lipidated amino acid uncouplers of mitochondria. *Cell* **166**, 424–435.
40 Tvrdik P, Asadi A, Kozak LP, Nedergaard J, Cannon B and Jacobsson A (1997) Cig30, a mouse member of a novel membrane protein gene family, is involved in the recruitment of brown adipose tissue. *J Biol Chem* **272**, 31738–31746.
41 Cannon B and Nedergaard J (2004) Brown adipose tissue: function and physiological significance. *Physiol Rev* **84**, 277–359.
42 Zhang Y, Zhang Y, Sun K, Meng Z and Chen L (2019) The SLC transporter in nutrient and metabolic sensing, regulation, and drug development. *J Mol Cell Biol* **11**, 1–13.
43 Wu Q, Kazantzis M, Doege H, Ortegon AM, Tsang B, Falcon A and Stahl A (2006) Fatty acid transport protein 1 is required for nonshivering thermogenesis in brown adipose tissue. *Diabetes* **55**, 3229–3237.
44 El Bacha T, Luz M and Da Poian A (2010) Dynamic adaptation of nutrient utilization in humans. *Nat Educ* **3**, 8.
45 Yoneshiro T, Wang Q, Tajima K, Matsushita M, Maki H, Igarashi K, Dai Z, White PJ, McGarrah RW, Ilkayeva OR *et al.* (2019) BCAA catabolism in brown fat controls energy homeostasis through SLC25A44. *Nature* **572**, 614–619.
46 Garcia RA, Roemmich JN and Claycombe KJ (2016) Evaluation of markers of beige adipocytes in white adipose tissue of the mouse. *Nutr Metab* **13**, 24.
47 Suwandhi L, Altun I, Karlina R, Miok V, Wiedemann T, Fischer D, Walzthoeni T, Lindner C, Böttcher A, Heinzmann SS *et al.* (2021) Asc-1 regulates white versus beige adipocyte fate in a subcutaneous stromal cell population. *Nat Commun* **12**, 1588.
48 de Koning TJ, Snell K, Duran M, Berger R, Poll-The BT and Surtees R (2003) L-serine in disease and development. *Biochem J* **371** (Pt 3), 653–661.
49 Lucas S, Chen G, Aras S and Wang J (2018) Serine catabolism is essential to maintain mitochondrial respiration in mammalian cells. *Life science alliance* **1**, e201800036.
50 McCarthy MJ (2014) Oxidative stress: a link between cardiovascular disease and psychiatric illness? *Acta Psychiatr Scand* **130**, 161–162.
51 Zhou X, He L, Wu C, Zhang Y, Wu X and Yin Y (2017) Serine alleviates oxidative stress via supporting glutathione synthesis and methionine cycle in mice. *Mol Nutr Food Res* **61**, 1700262.
52 Ducker GS and Rabinowitz JD (2017) One-carbon metabolism in health and disease. *Cell Metab* **25**, 27–42.
53 Fan J, Ye J, Kamphorst JJ, Shlomi T, Thompson CB and Rabinowitz JD (2014) Quantitative flux analysis reveals folate-dependent NADPH production. *Nature* **510**, 298–302.
54 Jörgensen JA, Zadravec D and Jacobsson A (2007) Norepinephrine and rosiglitazone synergistically induce Elovl3 expression in brown adipocytes. *Am J Physiol Endocrinol Metab* **293**, E1159–E1168.
55 de Jesus LA, Carvalho SD, Ribeiro MO, Schneider M, Kim SW, Harney JW, Larsen PR and Bianco AC (2001) The type 2 iodothyronine deiodinase is essential for adaptive thermogenesis in brown adipose tissue. *J Clin Investig* **108**, 1379–1385.
56 Rahbani JF, Roesler A, Hussain MF, Samborska B, Dykstra CB, Tsai L, Jedrychowski MP, Vergnes L, Reue K, Spiegelman BM *et al.* (2021) Creatine kinase B controls futile creatine cycling in thermogenic fat. *Nature* **590**, 480–485.
57 da Silva RP, Nissim I, Brosnan ME and Brosnan JT (2009) Creatine synthesis: hepatic metabolism of guanidinoacetate and creatine in the rat in vitro and in vivo. American journal of physiology. *Endocrinol Metab* **296**, E256–E261.
58 Jung RT, Shetty PS, James WP, Barrand MA and Callingham BA (1979) Reduced thermogenesis in obesity. *Nature* **279**, 322–323.
59 Rosenbaum M and Leibel RL (2010). Adaptive thermogenesis in humans. *Int J Obes* **34**, S47–S55.

Supporting information

Additional supporting information may be found online in the Supporting Information section at the end of the article.

Fig. S1. The gene-expression data based heat map shows the Pearson's correlation of 1049 genes expressed differentially in deep neck and subcutaneous derived preadipocytes and differentiated adipocytes.

Fig. S2. Effect of ASC-1 inhibitor (BMS-466442) on ASC-1 mRNA and protein expression in human neck area and SGBS adipocytes.
Fig. S3. Effect of ASC-1 inhibitor (BMS-466442) on cAMP stimulated OCR and ECAR in human SC neck and SGBS adipocytes.
Fig. S4. Effect of ASC-1 inhibitor (BMS-466442) on the mRNA expression of thermogenic marker genes in primary SC and DN adipocytes.
Fig. S5. Effect of ASC-1 inhibitor on the protein expression of mitochondrial complex subunits in SGBS adipocytes.
Fig. S6. The ASC-1 mRNA and protein expression in human neck tissue lysates.
Table S1. Genes primers and probes.
Table S2. Antibodies used in immunoblotting.
Supplementary Material